INTERNATIONAL JOURNAL OF HYDROGEN ENERGY XXX (2012) 1–9

Available online at www.sciencedirect.com

SciVerse ScienceDirect

journal homepage: www.elsevier.com/locate/he

Electrodeposited mesoporous platinum catalysts over hierarchical carbon monolithic support as anode in small PEM fuel cells

Mariano M. Bruno [a,b], *Esteban A. Franceschini* [a], *Federico A. Viva* [a], *Yohann R.J. Thomas* [a], *Horacio R. Corti* [a,*]

[a] *Grupo de Celdas de Combustible, Departamento de Física de la Materia Condensada, Centro Atómico Constituyentes, CNEA Av. General Paz 1499 (1650), San Martín, Buenos Aires, Argentina*

[b] *Escuela de Ciencia y Tecnología, Universidad de Gral. San Martín, Martin de Irigoyen 3100 (1650), San Martín, Buenos Aires, Argentina*

ARTICLE INFO

Article history:
Received 2 February 2012
Accepted 10 February 2012
Available online xxx

Keywords:
PEM
Fuel cells
Mesoporous catalyst
Hierarchical carbon

ABSTRACT

A mesoporous platinum catalyst was electrodeposited on the outer region of a carbon with hierarchical porous structure, using a block copolymer template. The platinum deposits exhibit an excellent stability enhanced by the roughness of the carbon support. Membrane Electrode Assemblies (MEAs) were prepared using the hierarchical carbon supported mesoporous platinum as anode, a Nafion 117 membrane, and a commercial gas diffusion electrode on the cathode side. Their performance was compared with that of MEAs prepared with commercial gas diffusion electrode and electrodeposited mesoporous catalyst over carbon cloth, by measuring the polarization curves in a single fuel cell (1 cm^2 active area) with H_2/O_2 at 60 °C and at ambient pressure. The fuel cell with mesoporous catalyst over hierarchical carbon reaches a power density of 25 mW $mgPt^{-1}$ cm^{-2}, 50% higher than that obtained with the commercial gas diffusion electrode. The high power density achieved is attributed to a synergic effect as a result of the integration of the structured catalyst and hierarchical carbon, which is proposed as an innovative procedure to prepare efficient MEAs for small fuel cells.

1. Introduction

Electronic portable devices such as, mobile phones, cameras, mp3 players, PDAs, netbooks [1–6] are increasingly more multi-functional, and consequently more power demanding. Alternative power sources for these modern devices, such as small fuel cells, needs to become more efficient and durable to replace current advanced batteries [6]. The component manufacturing and assembly procedures for small fuel cells cannot be extrapolated from macro fuel cells. Generally, the electrodes for fuel cells are obtained by spraying the catalyst ink directly onto the membrane or gas diffusion layer (GDL), forming the called gas diffusion electrode (GDE). This is a cumbersome method for small fuel cells fabrication, and new ones should be explored. In the trend to fabricate a small power supply based on PEM fuel cells, nanostructured materials are good candidates for innovative applications. Many efforts are being made to obtain a catalyst with high activity and long life [7,8]. However, the electrocatalyst activity is also affected by the accessibility of the gaseous or liquid reactants

* *Corresponding author*. Tel.: +5411 67727174; fax: +5411 67727121.
E-mail address: hrcorti@cnea.gov.ar (H.R. Corti).

0360-3199/$ – see front matter Copyright © 2012, Hydrogen Energy Publications, LLC. Published by Elsevier Ltd. All rights reserved.
doi:10.1016/j.ijhydene.2012.02.058

to the catalysts surface, the release of the reaction products, or the blocking of the catalyst electroactive area. Therefore, fuel cells performance could be improved beyond the intrinsic properties of the used materials by a suitable design and integration of the different components of the device. Thereby, structured materials with tailored properties are being proposed [9]. Over the past two decades, several routes to control those materials properties have arisen [10]. A recent study has shown that Pt mesoporous catalysts deposited on gold have higher performance than nanoparticled Pt catalysts supported on commercial carbon employing similar platinum load [11].

We have recently proposed the use of monolithic carbon with hierarchical pore size distribution as gas diffusion layer [9] in PEM fuel cells. The hierarchical monolithic carbon is formed by porous nanometer size spheres (whose packing generates mesopores), and straight capillaries crossing the bulk material. We expected that the gas transport through the capillaries be more efficient than through the mesopores. However, once the reactant gases reach the catalyst layer the flow could be redistributed in the lateral direction by the mesopores surrounding the capillaries.

The use of a viscous block copolymer as a template in the electrodeposition of Pt catalysts assure that the structured catalyst would be deposited only on the outer region of the carbon support, allowing the integration of the catalyst with the structured monolithic carbon which acts as gas diffusion layer and current collector [12]. Thus, we would avoid the use of the carbon powder support. Moreover, the electrodeposition process reduces the contact resistance between the GDL and the catalytic layer, also reducing its thickness, which in turns facilitates the contact of the catalyst with the membrane optimizing the three-phase zone [13]. Furthermore, the electrodeposition procedure replicates the surface shape of the gas diffusion layer reducing the problem on the imperfection of the interfacial contacts [14,15].

In the present work, the mesoporous platinum catalyst electrodeposited over hierarchical monolithic carbon was analyzed for the hydrogen oxidation reaction (HOR), aiming to the integration of the mentioned materials. In order to demonstrate such effects the performance of the integrated MEA was evaluated by measuring the fuel cell polarization curves with H_2/O_2 at 60 °C and compared with conventional MEAs.

2. Experimental part

2.1. Materials

2.1.1. Hierarchical porous carbon

The structure of the hierarchical carbon (HC) is formed by capillaries and nanopores. Two templates were used in the polymerization media to obtain pores of different sizes as described elsewhere [16]. Briefly, a precursor resin was prepared by polymerization of resorcinol (Fluka) and formaldehyde (Cicarelli, 37 wt.%). Na_2CO_3 (Cicarelli) was used as catalyst and poly(diallyldimethyl)ammonium chloride (PDADMAC, Sigma–Aldrich) as a structuring agent. The reactive mixture of resorcinol (R) and formaldehyde (F) was prepared in 0.4 M Na_2CO_3 (C) aqueous solution at 40 °C, stirring the mixture for 10 min and finally the PDADMAC (P) was added. The molar ratios of the components R:F:C:P were: 1:2:0.005:0.0212, respectively, where P is the monomeric unit. Once the mixture becomes homogenous, commercial polypropylene (PP; Softbond Inc.) cloths were immersed in the solution and heated at 70 °C for 48 h under atmospheric pressure. The resulting cubic shaped monolithic RF-polypropylene composite was dried in air for 5 days. After drying, laminar samples of the RF polymer were cut with a low speed saw (Isomet, Buehler). Finally, the samples were carbonized under nitrogen at 1000 °C at a heating rate of 60 °C h^{-1}. A typical monolithic carbon sample has an area of 5 cm^2 and a thickness of 300 μm.

2.1.2. Mesoporous platinum

Metal precursor solutions were prepared by mixing vigorously 1 g of Pluronic F127® with 1 cm^3 of 0.1 M hexachloroplatinic acid (HCPA) using a glass rod. The viscous mixture was poured in a purpose-built three electrode electrochemical cell having a carbon working electrode. A large surface area platinum was used as counter electrode, while an Ag/AgCl (sat) reference electrode was inserted in the mixture between the working and the counter electrodes. Galvanostatic reduction conditions (10 mA cm^{-2} for 30 min) were used to have an appropriated control of the mass of the electrodeposited catalysts. Both, hierarchical carbon and commercial carbon cloth were used as working electrodes in order to analyze the influence of the catalyst supports on the electrocatalytic activity. In Fig. 1 images of hierarchical carbon and carbon cloth before and after catalyst electrodepostion are shown. Residual compounds formed during the electrodeposition were removed from the Hierarchical Carbon–Mesoporous Catalyst (HCMC) and the Carbon Cloth–Mesoporous Catalyst (CCMC) systems by successive washes with water during 72 h. Finally, the samples were dried in a vacuum oven at 80 °C overnight. The masses of the electrodeposited catalysts were obtained by direct weighting of the electrodes before and after the electrodeposition. The average platinum electrodeposited masses were 0.50 ± 0.05 mg cm^{-2}.

2.2. Characterization

2.2.1. Morphology and structure of the materials

An ASAP 2020 (Micrometrics) instrument was used to measure the nitrogen adsorption isotherms at −196 °C. Specific surface area was calculated from the Brunauer–Emmett–Teller (BET) equation. The total volume of micropores (pores size smaller than 2 nm) was determined by applying the t-plot equation, and pore size distribution was calculated using Barret–Joyner–Halenda (BJH) equation from desorption branch isotherms [17].

Scanning electron microscope images were taken with a Quanta 200 (FEI Company) instrument. Scanning Electron Microscope (SEM) operating at a voltage of 25–30 kV, equipped with EDX. High-resolution electron micrographs were obtained using a Supra 40 (Zeiss Company) Field Emission Scanning Electron Microscopy (FESEM) operating at 3 kV.

X-ray Photoelectron Spectroscopy (XPS) measurements were performed under UHV conditions (base pressure

Please cite this article in press as: Bruno MM, et al., Electrodeposited mesoporous platinum catalysts over hierarchical carbon monolithic support as anode in small PEM fuel cells, International Journal of Hydrogen Energy (2012), doi:10.1016/j.ijhydene.2012.02.058

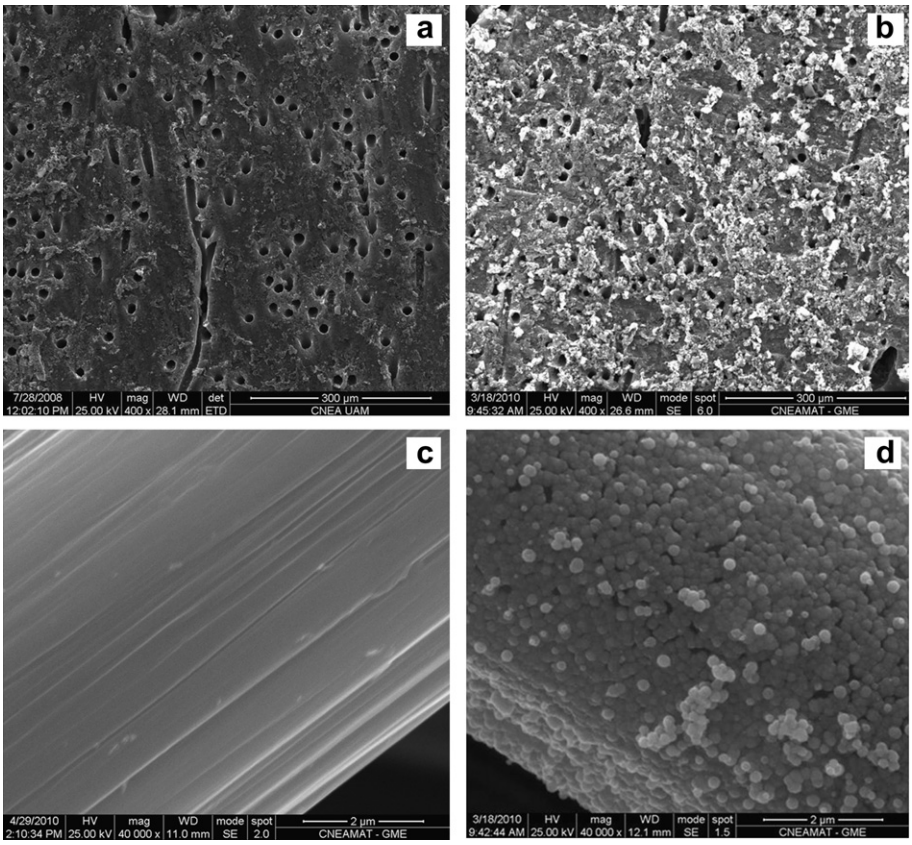

Fig. 1 – SEM images of de GDL with and without catalyst deposits. (a) Hierarchical carbon before electrodeposition and (b) after electrodepostion. (c) Carbon cloth before electrodeposition and (d) after electrodepostion.

$<5 \times 10^{-10}$ mbar) in a SPECS UHV spectrometer system equipped with a 150 mm mean radius hemispherical electron energy analyzer and a nine channeltron detector. XPS spectra were acquired at a constant pass energy of 20 eV using an unmonochromated Mg Kα (1253.6 eV) source operated at 12.5 kV and 20 mA and a detection angle of 30° with respect to the sample normal on grounded conducting substrates. Quoted binding energies are referred to the adventitious C 1s emission at 285 eV.

2.2.2. *MEAs preparation*

Three different MEAs having 1 cm^2 active area were prepared using the same electrolyte membrane and cathode electrode. The membrane used was Nafion® 117 (Ion Power), previously boiled in H_2O_2 3% (H_2O_2 30%, Biopack) followed by H_2SO_4 3% (95–97%, Merck). Gas Diffusion Electrodes (GDE) (Fuel Cell Store) composed of carbon cloth and a catalytic layer formed by Vulcan® carbon, Platinum particles and Nafion as binder (0.5 mg cm^{-2} of Pt) were used as cathode electrode. The three different anodes electrodes prepared and tested were: (i) mesoporous Pt catalyst electrodeposited over a hierarchical carbon (HCMC); (ii) mesoporous Pt catalyst electrodeposited over carbon cloth without PTFE treatment (hydrophilic) (CCMC); (iii) the same commercial gas diffusion electrode (CGDE) used as cathode electrode. After assembling the MEAs by hot pressing at 150 °C and 40 bar for 25 min., they were mounted into the fuel cell monostack manufactured *in house*, bolt tightened to 15 bar and re-humidified by water recirculation at 80 °C on the anodic and cathodic sides for 12 h. Linear Sweep polarization test were performed from open circuit voltage to a voltage close to short circuit (0.1 V). Humidified H_2 (RG 4.8, Indura) and O_2 (RG 4.8, Indura) were circulated at the anode and cathode, respectively, at a flow rate of 50 sccm. All measurements were performed with an Autolab PGSTAT302N potentiostat.

2.2.3. *Electrical in-plane resistivity of the GDL*

The electrical in-plane resistivity of HC material was determined using manual four point resistivity probing equipment with a SP4 four point probe head (Signatone Corporation). A current (200 μA) was applied with a current source (Keithley 6221) on the extreme contacts and the potential drop between central contacts was measured with a voltmeter (Keithley 2182A). According to Schroeder [18] the resistivity can be calculated according to the following equation,

$$\rho = \frac{\pi}{\ln(2)}\delta\left(\frac{V}{I}\right)f_1 f_2 \tag{1}$$

where f_1 and f_2 are correction factors for thickness and geometry of the sample, respectively, which can be written as:

$$f_1 = \frac{\ln(2)}{\ln\left(\frac{\sinh(\delta/s)}{\sinh(\delta/2s)}\right)} \tag{2}$$

Please cite this article in press as: Bruno MM, et al., Electrodeposited mesoporous platinum catalysts over hierarchical carbon monolithic support as anode in small PEM fuel cells, International Journal of Hydrogen Energy (2012), doi:10.1016/j.ijhydene.2012.02.058

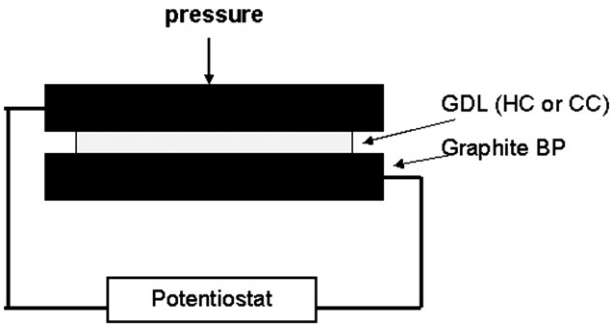

Fig. 2 – Schematic representation of the through-plane contact resistance arrangement.

$$f_2 = \frac{\ln(2)}{\ln(2) + \ln\left(\frac{(D/s)^2+3}{(D/s)^2-3}\right)} \quad (3)$$

with s the separation between each contact point (in our test $s = 1$ mm) and D the diameter of the sample. The resistivity of each sample was measured several times, with different locations of the probes on both faces of the HC material.

2.2.4. *GDL/bipolar plate electrical contact resistance*

Several authors have studied the electrical contact resistance in PEM fuel cells between GDL and stainless steel [19–21] or graphite [22,23] BP. As our fuel cell monostack was built with graphite BP, we choose to measure the contact resistance of this material with two different types of GDL (HC and CC) that have been used to make MEAs. As shown in Fig. 2 a piece of GDL was placed between two plates of graphite (AXF-5QCF from Poco Graphite, Inc.). This assembly was pressurized and the pressure was measured with a load cell (CZC-1000 from Reacción). A potential between −1 mV and +1 mV was applied with the Potentiostat and the current circulating through the assembly was measured. The total resistance was obtained from the slope of the current–voltage plot. The measured resistance, R_m, is then equal to:

$$R_m = R_s + 2R_{c,GDL/BP} + R_{b,GDL} \quad (4)$$

where R_s is the resistance of the peripherals system, which includes cables and multimeter resistances, $R_{c,GDL/BP}$ is the contact resistance between the GDL and the BP, and $R_{b,GDL}$ is the through-plane bulk resistance of the GDL, expressed as:

$$R_{b,CM} = \frac{\rho_{GDL} e_{GDL}}{A_{GDL}} \quad (5)$$

ρ_{GDL}, e_{GDL}, and A_{GDL} being the through-plane resistivity, the thickness and the area of the GDL, respectively. Eq. (4) can be reorganized,

$$R_m = R_s + \frac{1}{A_{GDL}}\left(2R'_{c,GDL/BP} + \rho_{GDL} e_{GDL}\right) \quad (6)$$

to obtain the contact resistance $R'_{c,GDL/BP} = A_{GDL} \cdot R_{c,GDL/BP}$

In order to separate the contribution of the contact resistance from the bulk resistance, some authors [24] used a method where the thickness of the sample is changed. In our case, we decided to change the contact area. Thus, measuring the resistances of two GDL having different areas, it is possible to determine the contact resistance through Eq. (6),

$$R'_{c,GDL/BP} = \frac{R_{m1} - R_{m2}}{2\left(\frac{1}{A_{GDL,1}} - \frac{1}{A_{GDL,2}}\right)} - \rho_{GDL} e_{GDL} \quad (7)$$

The thickness of the sample was determined with an accuracy of ±1 μm using a thickness meter (Köfer).

3. Results and discussion

3.1. *Hierarchical carbon characterization*

The nitrogen adsorption–desorption isotherms and pore size distribution of carbonized material at 1000 °C are shown in Fig. 3. An increase of the nitrogen adsorbed volume in the low relative pressure region and the hysteresis loop at high relative pressure can be seen in the isotherm (Fig. 3a). According to the IUPAC classification, the isotherm is of type-IV, and it has a hysteresis loop of type-H1. The analysis using the BET equation shows that a material with a high specific surface

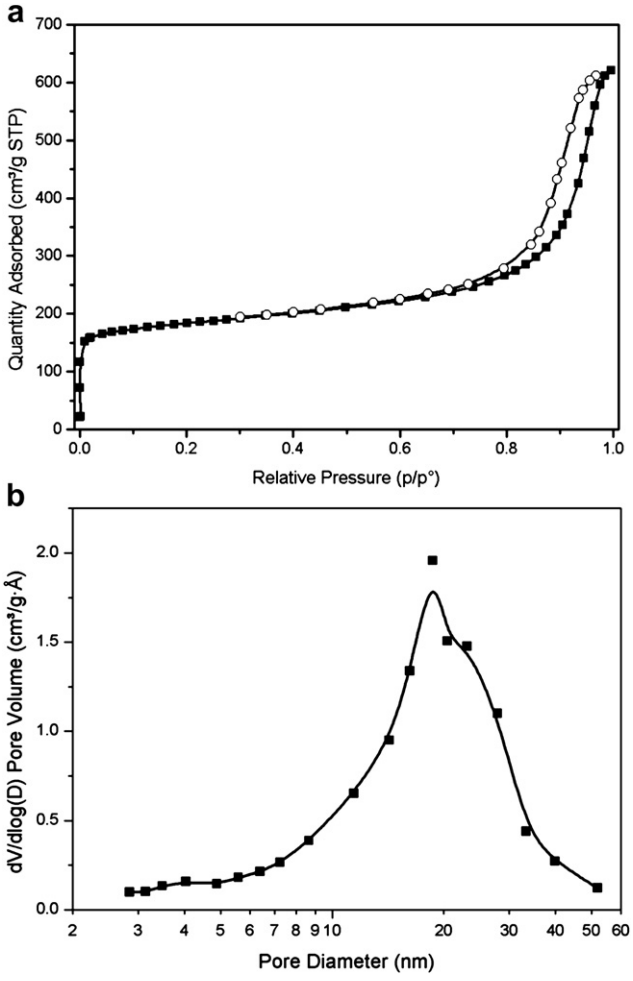

Fig. 3 – (a) N_2 adsorption isotherm of hierarchical carbon, (b) BJH pore size distribution (desorption branch) of a typical carbon sample.

Please cite this article in press as: Bruno MM, et al., Electrodeposited mesoporous platinum catalysts over hierarchical carbon monolithic support as anode in small PEM fuel cells, International Journal of Hydrogen Energy (2012), doi:10.1016/j.ijhydene.2012.02.058

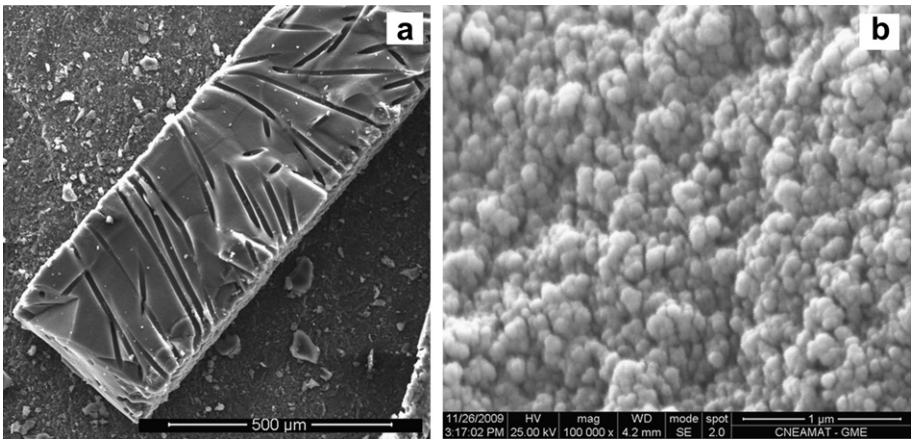

Fig. 4 – SEM images of the hierarchical carbon. (a) Side view, (b) top view at 100K× magnifications.

area (690 $m^2 g^{-1}$) was obtained. The type-H1 hysteresis loop at high relative pressure is indicative of mesoporous materials [17]. The total pore volume ($p/p^0 = 0.996$) is 0.96 $cm^3 g^{-1}$ and the micropore volume (*t*-plot) is 0.18 $cm^3 g^{-1}$. Fig. 3b shows the BJH pore size distribution (desorption branch) with a maximum around 20 nm.

SEM images of the final monolithic material are shown in Fig. 4. Capillaries of diameter around 15 μm, connecting both sides of the support, can be observed (Fig. 4a). Fig. 4b shows the monolithic surface formed by spherical particles smaller than 100 nm. According to previous work [25,26], the packing of these particles forms the porous structure (Fig. 4b). However, the high BET surface area of this material (690 $m^2 g^{-1}$) could not be accounted only from the surface of the spherical particles [25], suggesting that the achieved total surface area is the result of the clustering of smaller carbon nanoparticles, whose packing leads to micropores (<2 nm). Therefore, the material obtained has hierarchical pore structure (micro, meso and macro). As mentioned before, the surface density of capillaries can be easily controlled by adjusting the amount of the polypropylene template used in the fabrication method which gives an extra tuning on the macroporosity and weight of the final GDL [16]. The micropore structure provides anchoring sites to the catalyst while the mesopores and capillaries would improve the mass transport to/from the catalytic region.

An SEM image of the commercial carbon cloth used as GDL in the present work is shown in Fig. 5, to compare with the HC image of Fig. 1. The morphology of the material exhibits only macroporosity given by the carbon fiber array.

3.2. *Electrical resistivity and contact resistance results*

The measured in-plane resistivity of hierarchical carbon was 73 mΩ cm. The same value could be attributed for the through-plane resistivity, as this type of materials is isotropic [27]. For comparison, the CC used in this work has reported values of 9 and 132 mΩ cm for the in-plane and through-plane resistivities, respectively [28]. Those values indicate that HC has good electrical properties for its use as GDL in PEM fuel cells. However, it is well known that the major contribution to

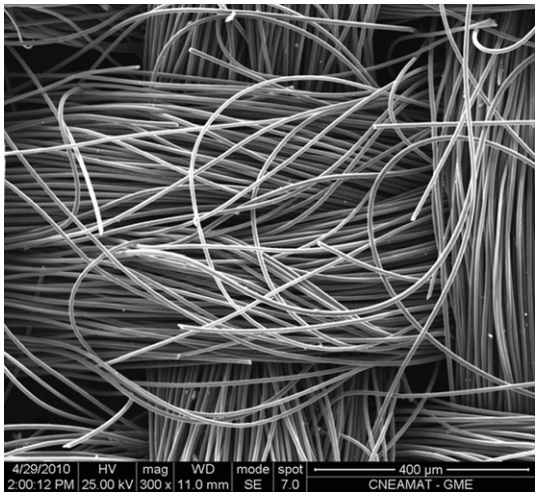

Fig. 5 – SEM images of carbon cloth.

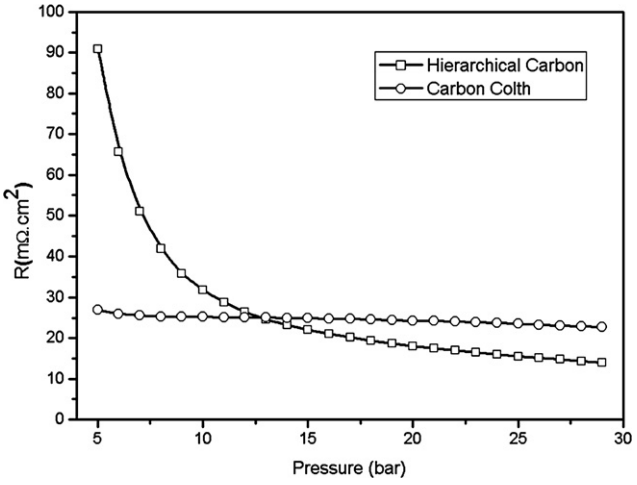

Fig 6 – Contact resistance curves for two GDL: HC and CC with graphite bipolar plates under pressures from 5 to 30 bar.

Please cite this article in press as: Bruno MM, et al., Electrodeposited mesoporous platinum catalysts over hierarchical carbon monolithic support as anode in small PEM fuel cells, International Journal of Hydrogen Energy (2012), doi:10.1016/j.ijhydene.2012.02.058

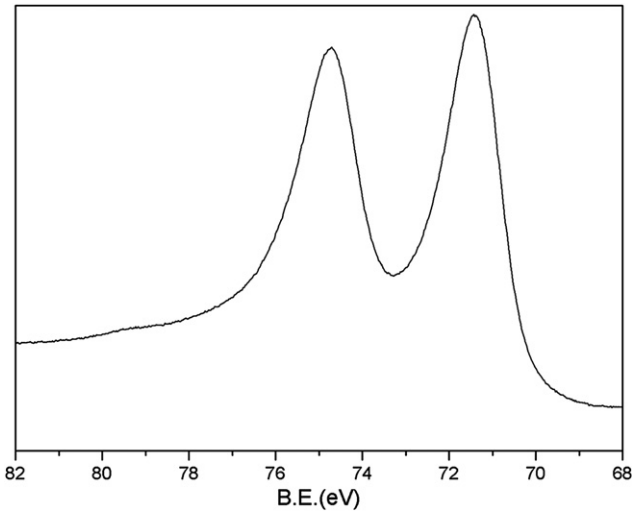

Fig. 7 – Pt 4*f* XPS spectra of the mesoporus Pt deposit over gold.

total electrical resistance is due to contact between components of the cell [24]. Fig. 6 shows the pressure dependence of the contact resistance between the graphite plate and two GDLs, HC and CC, where two different behaviors can be observed. For HC, the contact resistance is much higher at low pressures but decreases sharply and becomes lower than that of CC when the pressure is increased above 13 bar. Moreover, for CC the contact resistance is almost constant on the entire pressure range applied. These results are important because the fuel cell is usually assembled with clamping pressure ranging between 10 and 20 bar, to improve the cell performance [29]. The different behavior under pressure for both materials could be explained by a better contact of the HC due to a roughness decrease [14,15].

3.3. *Mesoporous catalyst characterization*

Survey XPS scans show the presence of Pt and the expected C and O contamination with no other elements being observed on the fresh catalyst. Thus XPS confirms the absence of metallic impurities. Fig. 7 shows the XP spectrum corresponding to the Pt 4*f* region, which consists of the expected doublet with binding energies of 71.2 eV (Pt $4f_{7/2}$) and 74.5 eV (Pt $4f_{5/2}$). The binding energy position reflects the oxidation state of platinum and it corresponds to metallic Pt. The presence of Pt oxides with Pt $4f_{7/2}$ peaks expected at binding energies greater than 72 eV are clearly negligible. and therefore it can be ruled out. Thus, XPS measurements show that the mesoporous films consist of pure metallic platinum.

The X-ray diffractogram of mesoporous platinum catalyst shows a Pt phase cell parameter of 3.92 ± 0.01 Å, in good agreement with data reported in the literature [30,31]. An average crystal size of 90 ± 10 Å was calculated using Scherrer's equation [32–34], which is consistent with previous works measurements [35]. The hexagonal structure of the mesoporous catalyst was proposed in a previous work based on the results of STM, FESEM and GISAXS analysis [35]. By comparing the FESEM images (Fig. 8) with those already reported [32] we concluded that the mesoporous hexagonal structure of the catalyst remain unchanged regardless of the type of support employed.

On the basis of the current time characteristic of the deposition, assuming a faradaic efficiency of 45% [35], the estimated upper limit thickness of the platinum film is around

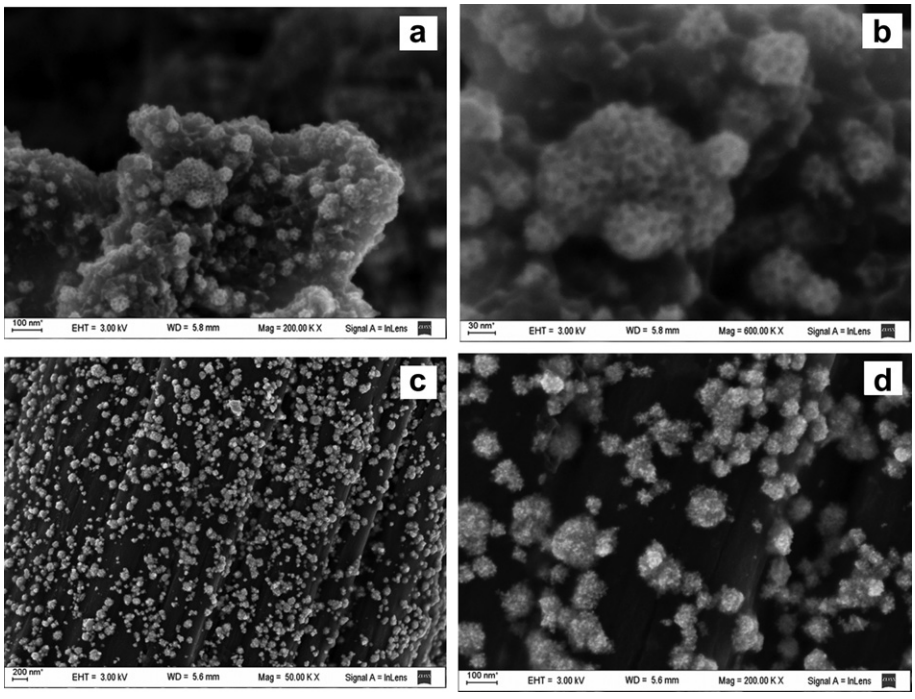

Fig. 8 – Image of platinum (white area) electrodeposited over (a, b) hierarchical carbon (black area) and (c, d) carbon cloth.

Please cite this article in press as: Bruno MM, et al., Electrodeposited mesoporous platinum catalysts over hierarchical carbon monolithic support as anode in small PEM fuel cells, International Journal of Hydrogen Energy (2012), doi:10.1016/j.ijhydene.2012.02.058

20 nm, but it should be lower than that due to the high real area of the electrode, and the partial surface coverage. Thus, the thickness of three-phase region in the HCMC MEA would be between 2 and 3 orders of magnitude smaller than the CGDE MEA.

3.4. *HCMC and CCMC characterization*

Fig. 8 shows FESEM images of CCMC and HCMC. High-resolution electron micrographs confirm that a mesoporous Pt structure, open and sponge-like, is formed on both substrates. It was previously reported that this catalyst layer is formed by porous spheres with a pore diameter of ~10 nm [35]. The spheres packing forms mesopores with a mosaic-like texture and defects located at the boundaries between domains, allowing a good accessibility of the hydrogen to the catalyst. This structure is very similar to the one observed in catalysts supported on gold plates [35] and, for this reason, we could infer that the support does not alter the structural properties of the catalyst.

Fig. 9a-d show the SEM images and Energy Dispersive X-Ray (EDX) mapping of platinum atoms over the CCMC and HCMC systems in order to analyze the distribution of the catalyst in the different carbon supports. The EDX mapping of CCMC in Fig. 9b shows a homogeneous distribution of the catalyst over the surface of the carbon cloth fibers. A similar distribution of catalyst was observed in HCMC. The white regions indicate the presence of the catalyst, while the dark ones correspond to areas where the catalyst is absent. Furthermore, the SEM image shown in Fig. 9d confirms that the capillaries remain open; although we cannot assure that the catalyst has not been deposited inside the walls of the capillaries.

The procedure of electrodeposition using a Pluronic F127® as template promotes the catalyst deposition on the outer region of the carbon support. At the same time, the mesoporous structure of the catalyst with good adherence was obtained independently of the carbonous substrate used, contrasting with the poor adherence of catalysts films and nanoparticles on carbon surfaces reported in the literature [36,37]. A high surface area for carbon materials represents an increment in the number of oxygenated superficial groups, playing an important role in enhancing the stability of the HCMC system [38]. However, is still not clear the mechanism of these groups for anchoring the catalysts nanoparticles [39]. For instance, the roughness, caused by the mesoporosity of the surface, also could provide good physical anchoring sites for the electrodeposited catalyst layer [40]. As discussed above, the nanoporous structure of the monolithic carbon makes the major contribution to its high surface area.

The employed electrodeposition procedure leaves most of the catalyst on the surface of the HC, as shown in Fig. 9d (EDX). In the MEA this surface is in direct contact with the membrane and therefore the interphase is optimized. On the other hand, in the CC the catalyst is distributed not only over the external fibers but also within them due to the inherent macroporosity, as shown in the Fig. 9b (EDX map). Therefore, not all the catalyst is available for electrochemical reaction. The decrease of the contact resistance with pressure between the HC/BP indicates that the rough surface became smoother increasing the area of contact as was observed previously Mench et al. [14,15].

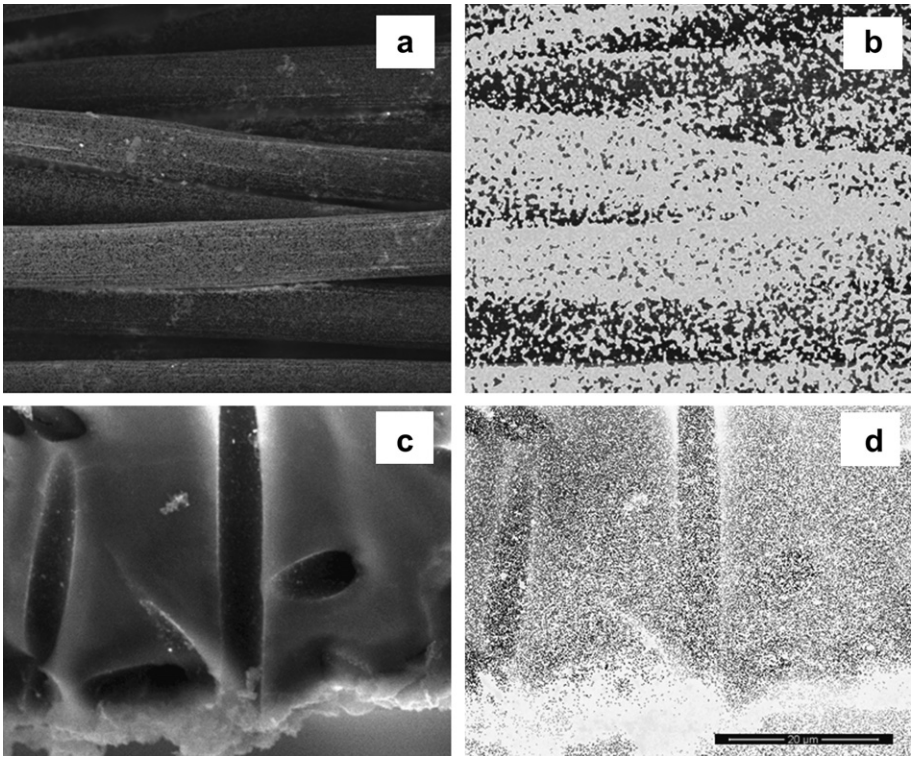

Fig. 9 – (a) SEM image and (b) EDX mapping of carbon cloth with the mesopores platinum deposit. (c) SEM image and (d) EDX mapping of hierarchical carbon with the mesopores platinum deposit.

Please cite this article in press as: Bruno MM, et al., Electrodeposited mesoporous platinum catalysts over hierarchical carbon monolithic support as anode in small PEM fuel cells, International Journal of Hydrogen Energy (2012), doi:10.1016/j.ijhydene.2012.02.058

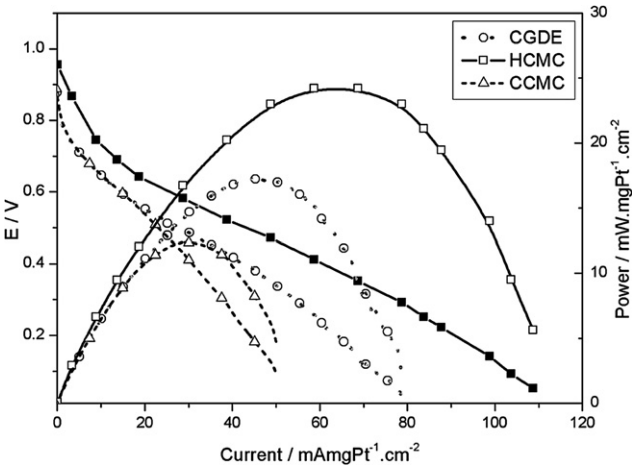

Fig. 10 – Mass normalized *I* vs *V* and power density curves of the single fuel cells with different MEAs at 60 °C. H_2 and O_2 flow rate 50 sccm.

3.5. *Fuel cell characterization*

In Fig. 10 the anode Pt mass normalized polarization and power curves for the three MEAs assembled are presented. The MEAs having the CCMC and the commercial electrode as anode show the same open circuit voltage (0.95 V) while the HCMC anode presents a slightly higher OCV (1.00 V), and its cell voltage keeps above the other two MEAs over the entire current sweep. Such results clearly indicate a lower activation polarization for the mesoporous catalyst deposited over the mesoporous carbon. On the other hand, CGDE and CCMC MEAs exhibit the same performance up to a voltage of 0.6 V, where the current density was 15 mA $mgPt^{-1}\,cm^{-2}$. At the same voltage HCMC presented a current density of 27 mA $mgPt^{-1}\,cm^{-2}$. As the current density is increased the potential decreases sharply for the CCMC MEA. Below 0.4 V, the mass transport effect was observed for CGDE. A peak power densities of 12.4 mW $mgPt^{-1}\,cm^{-2}$ was reached for CCMC and 17 mW $mgPt^{-1}\,cm^{-2}$ for CGDE. For the operation conditions used in the test, HCMC reached the best cell performance, with a peak power densities of 25 mW $mgPt^{-1}\,cm^{-2}$, that is, a power density 50% higher as compared to the commercial materials. Furthermore, mass transport effect for HCMC was observed at comparatively higher current than for CGDE.

4. Conclusions

Mesoporous Pt catalysts layers were prepared on hierarchical porous carbon and carbon cloth using a block copolymer (Pluronic F127®) as template. The structure of the hierarchical carbon support provides anchoring sites to the mesostructured Pt catalyst, increasing the surface density of nucleation centres.

The integration of structured materials shows the best performance in a fuel cell experiments, reaching a maximum power of 25 mW $mgPt^{-1}\,cm^{-2}$ at 60 °C. The obtained result might be due to a synergetic effect on the anodic global process through a suitable management of mass transport from/to the catalyst region. An additional improvement in the cell performance could be attributed to the reduction of the contact resistance decrease between the components. The contact resistance with the BP is lower for HC than CC under the clamping pressure (15 bar) used in the monostack FC.

In summary, all these results clearly indicate that the HCMC is a promising gas diffusion layer/catalyst support integrated device which could contribute to the miniaturization of small fuel cell for portable applications.

Acknowledgements

The authors thank financial support from Agencia Nacional de Promoción Científica y Tecnológica (PICT 2197 and PAE 36985), and CONICET (PIP 00095). We thank Federico Williams (INQUIMAE-UBA, Argentina) for helping us with the XPS analysis. Surface analysis characterization was performed in the Laboratorio de Microscopia Electrónica of CAC with the help of P. Bozzano, A. Dominguez and P. Reynoso Peitsch. HRC, MMB and FAV are permanent research fellow of CONICET. YRJT and EAF thank to CONICET for their fellowships.

REFERENCES

[1] Janssen MMP, Moolhuysen J. Platinum–tin catalysts for methanol fuel cells prepared by a novel immersion technique, by electrocodeposition and by alloying. Electrochim Acta 1976;21:869–78.
[2] Christensen PA, Hamnett A, MunkJ, Troughton GL. An in situ FTIR study of the electrochemical oxidation of methanol at small platinum particles. J Electroanal Chem 1994;370:251–8.
[3] Tripkovic AV, Popovic KD, Grgur BN, Blizanac B, Ross PN, Markovic NM. Methanol electrooxidation on supported Pt and PtRu catalysts in acid and alkaline solutions. Electrochim Acta 2002;47:3707–14.
[4] Snell KD, Keenan AG. Effect of anions and pH on the ethanol electro-oxidation at a platinum electrode. Electrochim Acta 1982;27:1683–96.
[5] de Tacconi NR, Lezna RO, Beden B, Hahn F, Lamy C. In-situ FTIR study of the electrocatalytic oxidation of ethanol at iridium and rhodium electrodes. J Electroanal Chem 1994; 379:329–37.
[6] de Lima RB, Paganin V, Iwasita T, Vielstich W. On the electrocatalysis of ethylene glycol oxidation. Electrochim Acta 2003;49:85–91.
[7] Antolini E. Platinum-based ternary catalysts for low temperature fuel cells. Part I. Preparation methods and structural characteristics. Appl Catal B Environ 2007;74: 324–36.
[8] Antolini E. Platinum-based ternary catalysts for low temperature fuel cells. Part II. Electrochemical properties. Appl Catal B Environ 2007;74:337–50.
[9] Bruno MM, Franceschini EA, Planes GA, Corti HR. Electrodeposited platinum catalysts over hierarchical carbon monolithic support. J Appl Electrochem 2010;40:257–63.

Please cite this article in press as: Bruno MM, et al., Electrodeposited mesoporous platinum catalysts over hierarchical carbon monolithic support as anode in small PEM fuel cells, International Journal of Hydrogen Energy (2012), doi:10.1016/j.ijhydene.2012.02.058

[10] Lu AH, Zhao D, Wan Y. Nanocasting: a versatile strategy for creating nanostructured porous materials. RSC Nanosci Nanotechnol; 2010.
[11] Planes GA, García G, Pastor E. High performance mesoporous Pt electrode for methanol electrooxidation. A DEMS study. Electrochem Commun 2007;9:839–44.
[12] Glora M, Wiener M, Petricevic R, Probstle H, Fricke J. Integration of carbon aerogels in PEM fuel cells. J Non-Cryst Solids 2001;285:283–7.
[13] Martín AJ, Chaparro AM, Gallardo B, Folgado MA, Daza L. Characterization and single cell testing of Pt/C electrodes prepared by electrodeposition. J Power Sources 2009;192: 14–20.
[14] Swamy T, Kumbur EC, Mench MM. Characterization of interfacial structure in PEFCs: water storage and contact resistance model. J Electrochem Soc 2010;157:B77–85.
[15] Swamy T, Kumbur EC, Mench MM. Investigation of bipolar plate and diffusion media interfacial structure in PEFCs: a fractal geometry approach. Electrochim Acta 2011;56: 3060–70.
[16] Bruno M, Corti HR, Balach J, Cotella NG, Barbero CA. Hierarchical porous materials capillaries in nanoporous carbon. Funct Mater Lett 2009;3:135–8.
[17] Rouquerol F, Rouquerol J, Sing K. Adsorption by powders and porous solids. San Diego: Academic Press; 1999.
[18] Schroeder DK. Semiconductor material and device characterization. John Wiley & Sons, Ltd; 1990.
[19] Wang H, Sweikart MA, Turner JA. Stainless steel as bipolar plate material for polymer electrolyte membrane fuel cells. J Power Sources 2003;115:243–51.
[20] Ismail MS, Damjanovic T, Ingham DB, Pourkashanian M, Westwood A. Effect of polytetrafluoroethylene-treatment and microporous layer-coating on the electrical conductivity of gas diffusion layers used in proton exchange membrane fuel cells. J Power Sources 2010;195:2700–8.
[21] Ihonen J, Jaouen F, Lindbergh G, Sundholm G. A novel polymer electrolyte fuel cell for laboratory investigations and in-situ contact resistance measurements. Electrochim Acta 2001;46:2899–911.
[22] Mishra V, Yang F, Pitchumani R. Measurement and prediction of electrical contact resistance between gas diffusion layers and bipolar plate for applications to PEM fuel cells. J Fuel Cell Sci Technol 2004;1:2–9.
[23] Nitta I, Hottinen T, Himanen O, Mikkola M. Inhomogeneous compression of PEMFC gas diffusion layer. Part I. Experimental. J Power Sources 2007;171:26–36.
[24] Mathias M, Roth J, Fleming J, Lehnert W. Chapter 46, Diffusion media materials and characterization. In: Handbook of fuel cells, fundamentals, technology and applications. Fuel cell technology and applications, vol. 3. John Wiley & Sons, Ltd; 2003.
[25] Bruno MM, Cotella NG, Miras MC, Barbero CA. A novel way to maintain resorcinol-formaldehyde porosity during drying: stabilization of the sol–gel nanostructure using a cationic polyelectrolyte. Colloid Surface A 2010;362:28–32.
[26] Yamamoto T, Mukai SR, Endo A, Nakaiwa M, Tamon H. Interpretation of structure formation during the sol-gel transition of a resorcinol-formaldehyde solution by population balance. J Colloid Interface Sci 2003;264:532–7.
[27] Jenkins GM, Kawamura K. Polymeric carbons-carbon fibre, glass and char. Cambridge University Press; 1976.
[28] Barbir F. PEM fuel cells: theory and practice. New York: Elsevier Academic Press; 2005.
[29] Chang WR, Hwang JJ, Weng FB, Chan SH. Effect of clamping pressure on the performance of a PEM fuel cell. J Power Sources 2007;166:149–54.
[30] Antolini E. Catalysts for direct ethanol fuel cells. J Power Sources 2007;170:1–12.
[31] Arico AS, Antonucci PL, Modica E, Baglio V, Kim H, Antonucci V. Effect of Pt–Ru alloy composition on high-temperature methanol electro-oxidation. Electrochim Acta 2002;47:3723–32.
[32] Li WZ, Zhou WZ, Li HQ, Zhou ZH, Zhou B, Sun GQ, et al. Nano-stuctured Pt–Fe/C as cathode catalyst in direct methanol fuel cell. Electrochim Acta 2004;49:1045–55.
[33] Tian ZQ, Jiang SP, Liang YM, Shen PK. Synthesis and characterization of platinum catalysts on multiwalled carbon nanotubes by intermittent microwave irradiation for fuel cell applications. J Phys Chem B 2006;110:5343–50.
[34] Hou Z, Yi B, Yu H, Lin Z, Zhang H. J. CO tolerance electrocatalyst of PtRu-HxMeO3/C (Me = W, Mo) made by composite support method. J Power Sources 2003;123:116–25.
[35] Franceschini EA, Planes GA, Williams FJ, Soler-Illia GJAA, Corti HR. Mesoporous Pt and Pt/Ru alloy electrocatalysts for methanol oxidation. J Power Sources 2011;196:1723–9.
[36] Etienne M, Walcarius A. Evaporation induced self-assembly of templated silica and organosilica thin films on various electrode surfaces. Electrochem Commun 2005;7:1449–56.
[37] Rodríguez-Reinoso F. The role of carbon materials in heterogeneous catalysis. Carbon 1998;36:159–75.
[38] Bleda-Martínez MJ, Lozano-Castelló D, Morallón E, Cazorla-Amorós D, Linares-Solano A. Chemical and electrochemical characterization of porous carbon materials. Carbon 2006;44: 2642–51.
[39] Fraga MA, Jordão E, Mendes MJ, Freitas MM, Faria JL, Figueiredo JL. Properties of carbon-supported platinum catalysts: role of carbon surface sites. J Catal 2002;209: 355–64.
[40] Viva FA, Bruno MM, Jobbágy M, Corti HR. electrochemical characterization of PtRu nanoparticles supported on mesoporous carbon for methanol electrooxidation. J Phys Chem C 2012;116:4097–104.

Please cite this article in press as: Bruno MM, et al., Electrodeposited mesoporous platinum catalysts over hierarchical carbon monolithic support as anode in small PEM fuel cells, International Journal of Hydrogen Energy (2012), doi:10.1016/j.ijhydene.2012.02.058